# Kinetics and Thermodynamics of the Formation of $MnFeP_4O_{12}$

**Banjong Boonchom*,†,‡ and Montree Thongkam‡**

King Mongkut's Institute of Technology Ladkrabang, Chumphon Campus, 17/1 M.6 Pha Thiew District, Chumphon, 86160, Thailand, and Department of Chemistry, Faculty of Science, King Mongkut's Institute of Technology Ladkrabang, Ladkrabang, Bangkok, 10520, Thailand

The kinetics and thermodynamics of dehydration and intermolecular polycondensation reactions of $Mn_{1/2}Fe_{1/2}(H_2PO_4)_2 \cdot H_2O$ and $Mn_{1/2}Fe_{1/2}(H_2PO_4)_2$ were studied under nonisothermal heating by thermogravimetry (TG). On the basis of three calculation procedures and 24 kinetic mechanism functions, kinetic triplets (*E*, *A*, kinetic model) using the Arrhenius equation were calculated for both processes. The comparison of the results obtained with these calculation procedures show a strong dependence on the selection of the mechanism function for the process. The thermodynamic functions ($\Delta H^*$, $C_p$, $\Delta G^*$, and $\Delta S^*$) of both reactions are calculated from differential scanning calorimetry (DSC) experiments. Kinetic and thermodynamic results indicate that the polycondensation step has a lower rate and is a stronger reaction than the dehydration step and corresponds to the breaking of the strong hydrogen-bonded P−OH group, in connection with the polycondensation reaction, which confirms that the decomposition product (manganese iron cyclotetraphosphate, $MnFeP_4O_{12}$) was obtained.

## Introduction

The cyclotetraphosphates of some bivalent metals are relatively stable compounds, both thermally and chemically.[1−5] This phosphate group exhibits properties of color anticorrosion ability and luminescence which allow their application as special inorganic pigments.[6−9] Additionally, they are a good source for macro- (P) and micronutrient (Ca, Mg, Fe, Mn, Co, Ni) fertilizers due to their solubility in soils. They are formed by the calcination of dihydrogenphosphates of bivalent metals or by the calcination of a mixture containing phosphorus and bivalent metal components in the corresponding ratio.[9−12] A number of papers have dealt with the use of thermal analysis (TA) under quasi-isothermal, quasi-isobaric conditions to follow the dehydration reactions of some binary metal dihydrogenphosphate hydrates.[13−15] So far, however, no report has appeared on the application of kinetic and thermodynamic methods to the investigation of the important condensation products, cyclotetraphosphates. The presence of water molecules of binary dihydrogenphosphate hydrates influences the intermolecular interactions (affecting the internal energy and enthalpy) as well as the crystalline disorder (entropy) and, hence, influences the free energy, thermodynamic activity, solubility, stability, and electrochemical and catalytic activity.[16−20] Studies on the thermodynamics, mechanisms, and kinetics of solid-state reactions are a challenging and difficult task with complexity resulting from a great variety of factors with diverse effects such as reconstruction of solid state crystal lattices, formation and growth of new crystallization nuclei, diffusion of gaseous reagents or reaction products, materials heat conductance, and static or dynamic character of the environment, physical state of the reagents—dispersity, layer thickness, specific area and porosity, type, amount, and distribution of the active centers on solid state surface, etc.[19−22] The results obtained from such studies can be directly applied in materials science for the preparation of various metals and alloys, cements, ceramics, glasses, enamels, glazes, polymers, and composite materials.[21−25]

The aim of the present paper is to study the kinetic and thermodynamic parameters of the formation of $MnFeP_4O_{12}$ from the decomposition of $Mn_{1/2}Fe_{1/2}(H_2PO_4)_2 \cdot H_2O$ and was followed using differential thermal analysis−thermogravimetry (TG/DTG/DTA), differential scanning calorimetry (DSC), X-ray powder diffraction (XRD), and Fourier transform-infrared (FT-IR) spectroscopy. This work seeks to characterize the thermal decomposition processes of $Mn_{1/2}Fe_{1/2}(H_2PO_4)_2 \cdot H_2O$, in relation to its thermodynamic ($\Delta H^*$, $C_p$, $\Delta S^*$, $\Delta G^*$) and kinetic (*E*, *A*, mechanism and model) properties, which are discussed for the first time.

## Experimental Section

The starting binary dihydrogenphosphate hydrate $Mn_{1/2}Fe_{1/2}(H_2PO_4)_2 \cdot H_2O$ (white−gray powder) was prepared in our laboratory from the Fe(c)−Mn(c)−$H_3PO_4$ system in a water−acetone medium at ambient temperature.[25] The qualities of the starting reactant and decomposition product were confirmed by atomic absorption spectroscopy (AAS, Perkin-Elmer, Analyst100), FTIR spectrophotometry (a Perkin-Elmer Spectrum GX FT-IR/FT-Raman spectrometer), X-ray diffraction analysis (a D8 Advanced powder diffractometer, Bruker AXS, Karlsruhe, Germany), and scanning electron microscopy.[25] Thermal analysis measurements (thermogravimetry, TG; differential thermogravimetry, DTG; and differential thermal analysis, DTA) were carried out by a Pyris Diamond Perkin-Elmer apparatus by increasing the temperature from (323 to 673) K with calcined α-$Al_2O_3$ powder as the standard reference. The experiments were performed in static air, at heating rates of (5, 10, 15, and 20) $K \cdot min^{-1}$. The sample mass was between (6.0 and 10.0) mg and placed into an alumina crucible without pressing. Differential scanning calorimetry was carried out for samples [(5 to 10) mg] in aluminum crucibles, over the temperature

* Corresponding author. Tel.: +66-7750-6422ext 4565. Fax: +66-7750-6410. E-mail address: kbbanjon@kmitl.ac.th.
† King Mongkut's Institute of Technology Ladkrabang, Chumphon Campus.
‡ Faculty of Science, King Mongkut's Institute of Technology Ladkrabang.

10.1021/je900310m CCC: $40.75 
Published on Web 09/16/2009

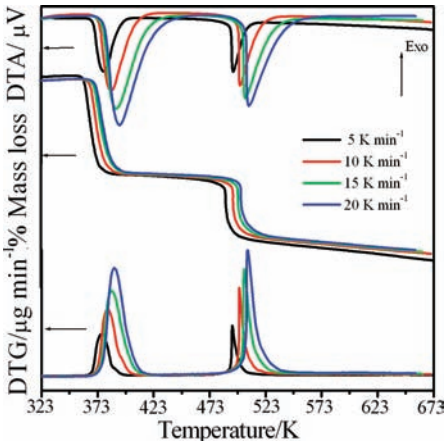


**Figure 1.** TG−DTG−DTA curves of $Mn_{1/2}Fe_{1/2}(H_2PO_4)_2 \cdot H_2O$ at different heating rates of (5, 10, 15, and 20) $K \cdot min^{-1}$ in dynamic dry air.

range of (303 to 823) K using differential scanning calorimetry (DSC) (Perkin-Elmer Pyris One). The heating rate employed was 10 $K \cdot min^{-1}$.

## Results and Discussion

***Sample Characterization.*** Figure 1 shows the TG−DTG−DTA curves of the thermal decomposition of $Mn_{1/2}Fe_{1/2}(H_2PO_4)_2 \cdot H_2O$ at four heating rates. TG curves of $Mn_{1/2}Fe_{1/2}(H_2PO_4)_2 \cdot H_2O$ show two clearly distinguishable mass loss stages in the range of (323 to 673) K. The two peaks in the DTG and DTA curves closely correspond to the mass loss observed on the TG trace. All TG−DTG−DTA curves are approximately the same shape, which indicates that the mass loss is independent of the heating rate. However, two decomposition stages were shifted toward higher temperatures when the heating rates increase. The eliminations of water are observed in two areas: (373 to 423) K and (473 to 673) K. The average corresponding observed mass losses of the four TG curves are (9.76 and 9.63) % by mass, which correspond to (1.50 and 1.48) mol of water, respectively. The total mass loss is 19.39 % (2.98 mol $H_2O$), which is in agreement with those reported for other binary dihydrogenphosphate dihydrates in the literature (1 < mole of water < 4).[11−14,25−27] The retained mass is about 80.64 % for all heating rates, compatible with the value expected for the formation of $MnFeP_4O_{12}$, which was verified by XRD measurement. The decomposition reactions of $Mn_{1/2}Fe_{1/2}(H_2PO_4)_2 \cdot H_2O$ are complex processes, which involve the dehydration of the coordinated water molecules (1 mol $H_2O$) and an intramolecular dehydration of the protonated phosphate groups (2 mol $H_2O$) as shown in eqs 1 and 2

$$Mn_{1/2}Fe_{1/2}(H_2PO_4)_2 \cdot H_2O \rightarrow Mn_{1/2}Fe_{1/2}(H_2PO_4)_2 + H_2O \quad (1)$$

$$Mn_{1/2}Fe_{1/2}(H_2PO_4)_2 \rightarrow 1/2MnFeP_4O_{12} + 2H_2O \quad (2)$$

An intermediate compound (acid polyphosphate, $Mn_{1/2}Fe_{1/2}(H_2PO_4)_2$) has been registered. The decomposed processes and the presented intermediates were similarly observed with other binary dihydrogen phosphates.[11−14,25] Manganese iron cyclotetraphosphate $MnFeP_4O_{12}$ was found to be the product of thermal decomposition at $T > 550$ K. To gain the complete decomposed $Mn_{1/2}Fe_{1/2}(H_2PO_4)_2 \cdot H_2O$, a sample of $Mn_{1/2}Fe_{1/2}(H_2PO_4)_2 \cdot H_2O$ was heated in a furnace at 573 K for 2 h.

The DSC curve of $Mn_{1/2}Fe_{1/2}(H_2PO_4)_2 \cdot H_2O$ (Figure 2) shows two endothermic peaks at (409 and 511) K (onset peak at (400, 506) K) which are due to the dehydration and the polycondensation reactions of this compound, respectively. The DSC peaks are in good agreement with DTG and DTA peaks as shown in Figure 1. According to the DSC curve, the heat of the dehydration and the polycondensation reactions can be calculated and are summarized in Table 1.

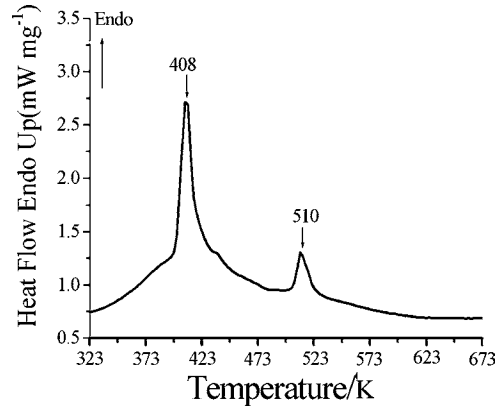


**Figure 2.** DSC curve of $Mn_{1/2}Fe_{1/2}(H_2PO_4)_2 \cdot H_2O$ at the heating rates of 10 $K \cdot min^{-1}$ in $N_2$ atmosphere.

**Table 1. Values of Thermodynamic Parameters for Two Decomposition Steps of $Mn_{1/2}Fe_{1/2}(H_2PO_2)_4 \cdot H_2O$ Calculated from DSC Data**

| parameter | dehydration | polycondensation |
|---|---|---|
| $T_1$(onset)/K | 399.89 | 505.79 |
| $T_p$/K | 409.44 | 511.57 |
| $T_2$(end)/K | 415.99 | 518.32 |
| $\Delta S$*/J·mol$^{-1}$·K$^{-1}$ | 74.42 | 11.85 |
| $C_p$/(J·mol$^{-1}$·K$^{-1}$) | 1885.01 | 484.20 |
| $\Delta H$*/J·mol$^{-1}$ | 30348.72 | 6066.98 |
| $\Delta G$*/J·mol$^{-1}$ | −121.04 | 4.35 |

The XRD patterns of $Mn_{1/2}Fe_{1/2}(H_2PO_4)_2 \cdot H_2O$ and its dehydration product ($MnFeP_4O_{12}$) are shown in Figure 3. In the systems of binary manganese iron solid solutions and individual metal dihydrogenphosphate (or metal cyclotetraphosphate), the electric charges of cations are equivalent, and the radii of cations are close to each other, so the spectrum peaks are quite similar.[11−14,25−27] Therefore, all detectable peaks are indexed as the $Mn(H_2PO_4)_2 \cdot 2H_2O$ and $Mn_2P_4O_{12}$ compounds with structure in standard data as PDF#350010 and PDF#380314, respectively. These results indicated that the two crystal structures are in the monoclinic system with space group $P2_1/n$ ($Z = 2$) for $Mn_{1/2}Fe_{1/2}(H_2PO_4)_2 \cdot H_2O$ and $C2/c$ ($Z = 4$) for $MnFeP_4O_{12}$.[25]

FT-IR spectra of $Mn_{1/2}Fe_{1/2}(H_2PO_4)_2 \cdot H_2O$ and its dehydration product ($MnFeP_4O_{12}$) are shown in Figure 4. Vibrational bands

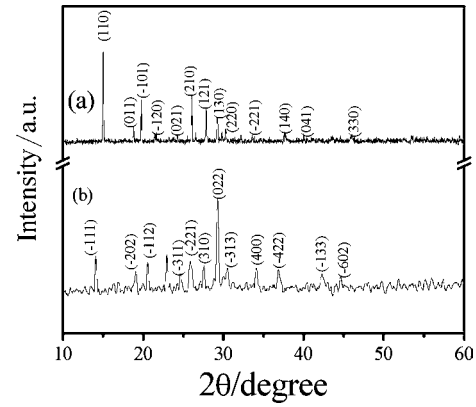


**Figure 3.** XRD patterns of (a) $Mn_{1/2}Fe_{1/2}(H_2PO_4)_2 \cdot H_2O$ and (b) $MnFeP_4O_{12}$.

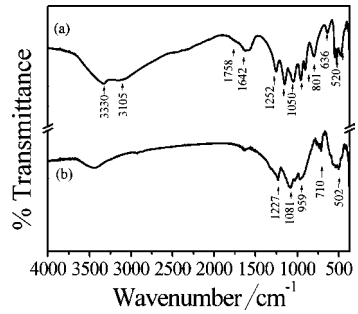


**Figure 4.** FT-IR spectra of (a) $Mn_{1/2}Fe_{1/2}(H_2PO_4)_2 \cdot H_2O$ and (b) $MnFeP_4O_{12}$.

are identified in relation to the crystal structure in terms of the fundamental vibrating units, namely, $H_2PO_4^-$ and $H_2O$, for $Mn_{1/2}Fe_{1/2}(H_2PO_4)_2 \cdot H_2O$ and the $[P_4O_{12}]^{4-}$ ion for $MnFeP_4O_{12}$, which are assigned according to the literature.[25−28] Vibrational bands of the $H_2PO_4^-$ ion are observed in the regions of (300 to 500, 700 to 900, 1160 to 900, 840 to 930, 1000 to 1200, and 2400 to 3300) $cm^{-1}$. These bands are assigned to the $\delta(O_2PO_2)$, $\gamma$(POH), $\delta$(POH), $\nu(PO_2(H_2))$, $\nu(PO_2)$, and $\nu$(OH) vibrations, respectively. The observed bands in the (1600 to 1700) $cm^{-1}$ and (3000 to 3500) $cm^{-1}$ regions are attributed to the water bending/C band and stretching vibrations/A band, respectively. Vibrational bands of the $[P_4O_{12}]^{4-}$ ion are observed in the ranges of (350 to 1220, 1150 to 1100, 1080 to 950, and 780 to 400) $cm^{-1}$. These bands can be assigned to the $\nu_{as}(OPO^-)$, $\nu_s(OPO^-)$, $\nu_{as}$(POP), and $\nu_s$(POP) vibrations, respectively. The observation of a strong $\nu_s$(POP) band is known to be the most striking feature of the cyclotetraphosphate spectra, along with the presence of the $\nu_{as}(OPO^-)$ band. From X-ray diffraction data,[27] it was shown that the crystal structure is monoclinic (space group $C2/c$) with a cyclic structure of the $[P_4O_{12}]^{4-}$ anion, which was confirmed by the FTIR measurements.

***Thermodynamics Parameters.*** Thermodynamic parameters, i.e., enthalpy change ($\Delta H^*$/J·mol$^{-1}$), heat capacity ($C_p$/J·mol$^{-1}$·K$^{-1}$), entropy change ($\Delta S^*$/J·mol$^{-1}$·K$^{-1}$), and Gibbs energy change ($\Delta G^*$/J·mol$^{-1}$), were calculated from the DSC experiment. The enthalpy change was calculated directly from the amount of heat change involved in each step per unit mass of the test sample. $\Delta H^*$ thus determined was implemented to calculate the specific heat capacity ($C_p$) using the following equation[29−31]

$$C_p = \frac{\Delta H}{\Delta T} \tag{3}$$

where $\Delta T = T_2 - T_1$; $T_1$ is the temperature at which the DSC peak begins to depart the baseline; and $T_2$ is the temperature at which the peak lands.[29,30] Subsequently, the changes of entropy ($\Delta S^*$) and Gibbs energy ($\Delta G^*$) were calculated using the following equations[29−31]

$$\Delta S^* = 2.303 C_p \log \frac{T_2}{T_1} \tag{4}$$

$$\Delta G^* = \Delta H^* - T_p \Delta S^* \tag{5}$$

On the basis of the DSC data, the values of $\Delta H^*$, $\Delta S^*$, $C_p$, and $\Delta G^*$ for the activated complex formation from the reagent can be calculated according to eqs 3, 4, and 5 and are presented in Table 1.

The formation of the activated complex of the reagent reflects in a specific way the change of the entropy ($\Delta S^*$). As can be seen from Table 1, the entropy of activation ($\Delta S^*$) values for the first and second steps are positive. A positive entropy value indicates that the transition state is highly disordered compared with the initial state. It means that the corresponding activated complexes have a lower degree of arrangement than the initial state. Since the decomposition of $Mn_{1/2}Fe_{1/2}(H_2PO_4)_2 \cdot H_2O$ proceeds as two consecutive reactions, the formation of the second activated complex passed in situ. In terms of the theory of activated complexes (transition theory),[31−35] a positive value of $\Delta S^*$ indicates a malleable activated complex that leads to a large number of degrees of freedom of rotation and vibration. The result may be interpreted as a "fast" stage. On the other hand, a negative value of $\Delta S^*$ indicates a highly ordered activated complex, and the degrees of freedom of rotation as well as of vibration are less than they are in the nonactivated complex. This result may indicate a "slow" stage.[33−35] Therefore, the first and second steps of the thermal decomposition of $Mn_{1/2}Fe_{1/2}(H_2PO_4)_2 \cdot H_2O$ may be interpreted as "fast" stages. On the other hand, the $\Delta S^*$ value observed for the polycondensation step was lower than that of the dehydration step, which is due to the necessity of more significant rearrangement in the $Mn_{1/2}Fe_{1/2}(H_2PO_4)_2$ structure because the strength of the bond between cation and anion is predominantly ionic. According to our interpretation, in these cases the bonds would be strong (large values of $E$), and more rearrangement would be necessary (large absolute values of $\Delta S^*$) to break them for the formation of the activated complex of the reagent. For the enthalpy $\Delta H^*$, positive values are in good agreement with two endothermic effects in the DTA and DSC data. The negative and positive values of $\Delta G^*$ indicate spontaneous and nonspontaneous processes for the dehydration and polycondensation stages, respectively. The $\Delta G^*$ values indicate that the second step needs a higher-energy pathway than the first step. That means that the rate of the second step is lower than that of the first step of the dehydration and indicates that the second decomposition step occurs with more difficulty than the first decomposition step according to the breaking of the strong hydrogen-bonded P−OH group in this structure.

***Kinetic Parameters.*** Kinetic analysis of heterogeneous solid-state reactions always starts with the general formula for the reaction:[16−24] A (solid) → B (solid) + C (gas). The kinetics of such reactions is described by various equations taking into account the special features of their mechanisms. The reaction can be expressed through the temperatures corresponding to fixed values of the extent of conversion ($\alpha = (m_i - m_t)/(m_t - m_f)$, where $m_i$, $m_t$, and $m_f$ are the initial, current, and final sample mass, at moment time $t$) from experiments at different heating rates ($\beta$).

$$\frac{d\alpha}{dt} = k(T) f(\alpha) \tag{6}$$

The temperature dependence of the rate constant $k$ for the process is described by the Arrhenius equation

$$k = A \exp\left(-\frac{E}{RT}\right) \tag{7}$$

where $A$ is the pre-exponential factor ($s^{-1}$); $E$ is the apparent activation energy (kJ·mol$^{-1}$); $T$ is the absolute temperature (K); and $R$ is the gas constant (8.314 J·mol$^{-1}$·K$^{-1}$). Substitution of eq 7 in eq 6 gives

$$\frac{d\alpha}{dt} = A \exp\left(-\frac{E}{RT}\right) f(\alpha) \tag{8}$$

When the temperature increases at a constant rate

$$\frac{dT}{dt} = \beta = \text{const} \tag{9}$$

Therefore

$$\frac{d\alpha}{dT} = \frac{A}{\beta}\exp\left(-\frac{E}{RT}\right)f(\alpha) \quad (10)$$

The conversion function $f(\alpha)$ for a solid-state reaction depends on the reaction mechanism. The solutions on the left-hand side integral depend on the explicit expression of the function $f(\alpha)$ and are denoted as $g(\alpha)$. The formal expressions of the functions $g(\alpha)$ depend on the conversion mechanism and its mathematical model. The latter usually represents the limiting stage of the reaction—the chemical reactions; random nucleation and nuclei growth; phase boundary reaction or diffusion. Algebraic expressions of functions of the most common reaction mechanisms operating in solid-state reactions are presented in the literature.[17−20]

Several authors[16−24] have suggested different ways to solve the right-hand side integral. The integral methods of the Coats−Redfern (CR),[36] the Madhysudanan−Krishnan−Ninan (MKN),[37] and the Tang et al. (TL)[38] have been predominantly and successfully used for studying the kinetics of dehydration and decomposition of different solid substances.[16−24] For the present study, calculation procedures were based on the CR, MKN, and TL equations. Data from the TG curves in the decomposition range $0.1 < \alpha < 0.9$ were used to determine the kinetic parameters of the process in all used calculation procedures.

The Coats and Redfern (CR) equation[36]

$$\ln\left(\frac{g(\alpha)}{T^2}\right) = \ln\left(\frac{AR}{\beta E_\alpha}\right)\left(1 - \frac{2RT}{E_\alpha}\right) - \left(\frac{E_\alpha}{RT}\right) \cong \ln\left(\frac{AR}{\beta E_\alpha}\right) - \left(\frac{E_\alpha}{RT}\right) \quad (11)$$

The Madhysudanan−Krishnan−Ninan (MKN) equation[37]

$$\ln\frac{g(\alpha)}{T^{1.921503}} = \left[\ln\frac{AE}{\beta R} + 3.772050 - 1.921503\ln E\right] - 0.120394\frac{E}{T} \quad (12)$$

Tang et al. (TL) equation[38]

$$\ln\frac{g(\alpha)}{T^{1.894661}} = \left[\ln\frac{AE}{\beta R} + 3.63504095 - 1.894661\ln E\right] - 1.00145033\frac{E}{RT} \quad (13)$$

These equations were used to estimate the most correct mechanism, i.e., $g(\alpha)$ and $f(\alpha)$ functions. The activation energy, pre-exponential factor, and the correlation coefficient can be calculated from the CR (eq 11), MKN (eq 12), and TL (eq 13) equations combined with 24 conversion functions (Table 2).[16−20] Equations 10 to 12 imply that there are differences in the calculated values of the activation energy and pre-exponential factor $A$ in the Arrhenius equation, even with the same $g(\alpha)$ function. The value of the coefficient of determination in the linear regression $R^2$ for eqs 11 to 13 was used as a criterion for

**Table 2. Algebraic Expressions of Functions $g(\alpha)$ and $f(\alpha)$ and Their Corresponding Mechanism[16−20]**

| no. | symbol | name of the function | $f(\alpha)$ | $g(\alpha)$ | rate-determination mechanism |
|---|---|---|---|---|---|
| | | | 1. Chemical Process of Mechanism Noninvoking Equations | | |
| 1 | $F_{1/3}$ | one-third order | $(3/2)(1-\alpha)^{2/3}$ | $[1-(1-\alpha)^{1/3}]$ | chemical reaction |
| 2 | $F_{3/4}$ | three-quarters order | $4(1-\alpha)^{3/4}$ | $[1-(1-\alpha)^{1/4}]$ | chemical reaction |
| 3 | $F_{3/2}$ | one and a halt order | $2(1-\alpha)^{3/2}$ | $[1-(1-\alpha)^{-1/2}-1]$ | chemical reaction |
| 4 | $F_2$ | second order | $(1-\alpha)^2$ | $(1-\alpha)^{-1}-1$ | chemical reaction |
| 5 | $F_n$ | $n$th-order kinetics ($n \pm 1$) | $(1-\alpha)^n$ | $[1-(1-\alpha)^{1-n}]/(1-n)$ | chemical reaction |
| | | | 2. Acceleratory Equations | | |
| 6 | $P_{3/2}$ | Mampel power law | $(2/3)\alpha^{-1/2}$ | $\alpha^{3/2}$ | nucleation |
| 7 | $P_{1/2}$ | Mampel power law | $2\alpha^{1/2}$ | $\alpha^{1/2}$ | nucleation |
| 8 | $P_{1/3}$ | Mampel power law | $3\alpha^{2/3}$ | $\alpha^{1/3}$ | nucleation |
| 9 | $P_{1/4}$ | Mampel power law | $4\alpha^{3/4}$ | $\alpha^{1/4}$ | nucleation |
| | | | 3. Sigmoid Rate Equations or Random Nucleation and Subsequent Growth | | |
| 10 | $A_1$, $F_1$ | Avrami−Erofeev equation | $(1-\alpha)$ | $-\ln(1-\alpha)$ | assumed random nucleation and its subsequent growth, $n = 1$ |
| 11 | $A_{3/2}$ | Avrami−Erofeev equation | $(3/2)(1-\alpha)[-\ln(1-\alpha)]^{1/3}$ | $[-\ln(1-\alpha)]^{2/3}$ | assumed random nucleation and its subsequent growth, $n = 1.5$ |
| 12 | $A_2$ | Avrami−Erofeev equation | $2(1-\alpha)[-\ln(1-\alpha)]^{1/2}$ | $[-\ln(1-\alpha)]^{1/2}$ | assumed random nucleation and its subsequent growth, $n = 2$ |
| 13 | $A_3$ | Avrami−Erofeev equation | $3(1-\alpha)[-\ln(1-\alpha)]^{2/3}$ | $[-\ln(1-\alpha)]^{1/3}$ | assumed random nucleation and its subsequent growth, $n = 3$ |
| 14 | $A_4$ | Avrami−Erofeev equation | $4(1-\alpha)[-\ln(1-\alpha)]^{3/4}$ | $[-\ln(1-\alpha)]^{1/4}$ | assumed random nucleation and its subsequent growth, $n = 4$ |
| | | | 4. Deceleratory Rate Equations | | |
| | | | 4.1 Phase Boundary Reaction | | |
| 15 | $R_1$, $F_0$, $P_1$ | Power law | $(1-\alpha)^0$ | $\alpha$ | one-dimensional advance of the reaction interface, power law or zero-order kinetics |
| 16 | $R_2$, $F_{1/2}$ | Power law | $2(1-\alpha)^{1/2}$ | $[1-(1-\alpha)^{1/2}]$ | contracting area (cylindrical symmetry) or one-half-order |
| 17 | $R_3$, $F_{2/3}$ | Power law | $3(1-\alpha)^{2/3}$ | $[1-\ln(1-\alpha)]^{1/3}$ | Contracting volume (spherical symmetry) or two-thirds order |
| | | | 4.2 Based on the Diffusion | | |
| 18 | $D_1$ | Parabola law ($\alpha = kt^{1/2}$) | $1/2\alpha$ | $\alpha^2$ | One-dimension diffusion |
| 19 | $D_2$ | Valensi equation | $[-\ln(1-\alpha)]^{-1}$ | $\alpha + (1-\alpha)\ln(1-\alpha)$ | Two-dimension diffusion |
| 20 | $D_3$ | Jander equation | $(3/2)(1-\alpha)^{2/3}/[1-(1-\alpha)^{1/3}]$ | $[1-(1-\alpha)^{1/3}]^2$ | Three-dimension diffusion |
| 21 | $D_4$ | Ginstling−Brounstein equation | $(3/2)(1-\alpha)^{-1/3}-1]^{-1}$ | $[1-(2/3)\alpha-(1-\alpha)^{2/3}]$ | Three-dimension diffusion |
| 22 | $D_5$ | Zhuravlev−Lesokhin−Tempelman equation | $(3/2)(1-\alpha)^{4/3}/[1-(1-\alpha)^{-1/3}]$ | $[(1-\alpha)^{-1/3}-1]^2$ | Three-dimension diffusion |
| 23 | $D_6$ | Komastsu−Uemura or anti-Jander equation | $(3/2)(1+\alpha)^{2/3}/[(1+\alpha)^{1/3}-1]$ | $[(1+\alpha)^{1/3}-1]^2$ | Three-dimension diffusion |
| 24 | $D_7$ | Anti−Ginstling−Brounstein equation | $(3/2)/[(1+\alpha)^{-1/3}-1]$ | $[1+(2/3)\alpha-(1+\alpha)^{2/3}]$ | Three-dimension diffusion |

**Table 3. Values of Kinetic Parameters for Two Decomposition Steps of $Mn_{1/2}Fe_{1/2}(H_2PO_2)_4 \cdot H_2O$ Calculated from TG Data using Different Methods**

| parameter | calculation procedure | | |
|---|---|---|---|
| | CR | MKN | TL |
| | Dehydration of $Mn_{1/2}Fe_{1/2}(H_2PO_2)_4 \cdot H_2O$ | | |
| kinetic model | $F_{3/2}$ | $F_{3/2}$ | $F_{3/2}$ |
| $R^2$ | 0.99652 | 0.99653 | 0.99654 |
| $E$/kJ·mol$^{-1}$ | 136.48 | 136.73 | 136.75 |
| $A$/min$^{-1}$ | $1.87 \cdot 10^{21}$ | $2.01 \cdot 10^{21}$ | $2.02 \cdot 10^{21}$ |
| | Deprotonated Hydrogen Phosphate of $Mn_{1/2}Fe_{1/2}(H_2PO_2)_4$ | | |
| kinetic model | $D_5$ | $D_5$ | $D_5$ |
| $R^2$ | 0.97495 | 0.97502 | 0.97505 |
| $E$/kJ·mol$^{-1}$ | 244.45 | 244.55 | 244.55 |
| $A$/min$^{-1}$ | $2.26 \cdot 10^{31}$ | $4.00 \cdot 10^{31}$ | $2.34 \cdot 10^{31}$ |

the estimation of the three calculating procedures aiming to find the most suitable one. For the calculations of the kinetic parameters, a computer program was developed for all the data manipulations.

At the constant condition of other parameters, the TG curves for dehydration and decomposition of $Mn_{1/2}Fe_{1/2}(H_2PO_4)_2 \cdot H_2O$ in dynamic dry air at various heating rates [(5, 10, 15, and 20) K·min$^{-1}$] are shown in Figure 1. According to the CR, MKN, and TL methods, the basic data of $\alpha$ and $T$ collected from Figure 1 are illustrated in Table 3. These data were processed according to the three calculation procedures and the kinetic equations shown in Table 2, aiming to obtain a maximum value of the coefficient of determination $R^2$ (Table 3). As can see from Table 3, the possible conversion function of the dehydration reaction is $F_{3/2}$ (three-halves kinetic order), which has a higher coefficient of determination than the other functions. Thus, it can be stated that the mechanism function with integral $g(\alpha) = 2[(1 - \alpha)^{1/2} - 1]$ and differential form $f(\alpha) = (1 - \alpha)^{3/2}$ belongs to the mechanism of chemical decomposition reaction (mechanism noninvoking equation). Concerning the second step of decomposition, the better coefficient of determination was obtained with mechanism function $D_5$ (Zhuravlev, Lesokin, Tempelman equation), which corresponds to three-dimensional diffusion with integral $g(\alpha) = [(1 - \alpha)^{-1/3} - 1]^2$ and differential form $f(\alpha) = (3/2)(1 - \alpha)^{4/3}((1 - \alpha)^{-1/3} - 1)^{-1}$. The values of the correlation coefficient and kinetic triplets ($E$, $A$, kinetic model) obtained with the three equations were quite close which did give enough grounds to select the most suitable kinetic function model. These were considered enough to conclude that the kinetic triplet parameters of nonisothermal decomposition of $Mn_{1/2}Fe_{1/2}(H_2PO_4)_2 \cdot H_2O$ can be reliably calculated with the correctly chosen $g(\alpha)$ function. However, the kinetic triplet parameters of the two decomposition processes are different. The dehydration reaction of $Mn_{1/2}Fe_{1/2}(H_2PO_4)_2 \cdot H_2O$, however, is characterized by significantly lower values of $E_a$ and $A$ compared to the polycondensation reaction relative to the formation of an intermediary higher molecular mass compound. Similar tendency is observed in the kinetics of dehydration and decomposition of $Mn(H_2PO_4)_2 \cdot 2H_2O$.[39] When solid-state reactions of the same type occur, it was found that large values of $A$ correspond to large values of $E$. The large $E$ values are usually connected with the higher strength of the chemical bond (bonds) which is to be broken. The significantly lower values of $E$ and $A$ observed for thermal dehydration of $Mn_{1/2}Fe_{1/2}(H_2PO_4)_2 \cdot H_2O$ compared to those of thermal decomposition of $Mn_{1/2}Fe_{1/2}(H_2PO_4)_2$ showed that the bond strength between $H_2O$ molecules, cations, and anions was lower than that between cations ($Mn^{2+}$, $Fe^{2+}$) and anions ($H_2PO_4^-$ ion). This was confirmed from the higher temperature of the decomposition stage (Figure 1), which indicates that the presence of very strong hydrogen bonds of $Mn_{1/2}Fe_{1/2}(H_2PO_4)_2$ is higher than that of $Mn_{1/2}Fe_{1/2}(H_2PO_4)_2 \cdot H_2O$. The result is consistent with the TG/DTG/DTA (the true scheme 1 and 2) and DSC results, which explains the elimination of water molecules in crystallohydrate for the first step and the elimination of water molecules from dihydrogenphosphate ion for the second step. The big difference between the values of the pre-exponential factor $A$ for the processes of dehydration and decomposition of the studied compound is interesting. The values of the pre-exponential factor $A$ in the Arrhenius equation for solid phase reactions are expected to be quite wide ranged (6 or 7 orders of magnitude), even after the correction of the surface area effect.[40,41] The empirical first-order pre-exponential factors may vary from ($10^5$ to $10^{18}$) s$^{-1}$. The low factors will often indicate a surface reaction, but if the reactions are not dependent on the surface area, the low factor may indicate a "tight" complex. The high factors will usually indicate a "loose" complex. Even higher factors (after correction of the surface area) can be obtained if the complexes have free transition on the surface. Since the concentrations in solids are not controllable in many cases, it would be convenient if the magnitude of the pre-exponential gives an indication of the reaction molecularity. This appears to be true only for nonsurface-controlled actions having low (<$10^9$ s$^{-1}$) pre-exponential factors. On the basis of these reasons, the first and second steps of the thermal decomposition of $Mn_{1/2}Fe_{1/2}(H_2PO_4)_2 \cdot H_2O$ may be interpreted as loose complexes. This may most likely occur on a surface where the complex extends itself from the surface and perhaps rotates parallel to the surface. For this unimolecular case, the complex is expected to expand in size and hence interact more intensely with its neighbors. On the basis of the results, the thermal analysis and kinetic and thermodynamic results are consistent and indicate the breaking bonds of water molecules and a true P−OH, in connection with the polycondensation reaction,[11−14,39] which confirm that the decomposition product, manganese iron cyclotetraphosphate $MnFeP_4O_{12}$, was obtained.

## Conclusions

On the basis of the studies carried out, the thermal decomposition of $Mn_{1/2}Fe_{1/2}(H_2PO_4)_2 \cdot H_2O$ was found to occur in two processes: the dehydration and the deprotonated dihydrogenphosphate reactions. The dehydration reaction of $Mn_{1/2}Fe_{1/2}(H_2PO_4)_2 \cdot H_2O$ involves the elimination of water molecules of crystallohydrate, while the deprotonated dihydrogenphosphate reaction of $Mn_{1/2}Fe_{1/2}(H_2PO_4)_2$ involves the breaking bond of a true P−OH and polycondensation reaction of phosphate groups. The parameters characterizing the kinetics and thermodynamics of two thermal transformation reactions of the studied compound were different because the nature of chemical units (cation, anion, and water molecules) exerts significant effects on electron density and, hence, on the strength of its bond to structure. On

the basis of correctly established values of the apparent activation energy, pre-exponential factor, and the changes of entropy, enthalpy, and Gibbs energy, certain conclusions can be made concerning the mechanisms and characteristics of the processes. The results can be applied to the production of $MnFeP_4O_{12}$, which plays a large role in industrial applications.

**Acknowledgment**

The authors would like to thank the Chemistry Department, Khon Kaen University for facilities.

## Literature Cited

(1) Trojan, M.; Šulcová, P.; Sýkorová, L. Thermal Analysis of Ba(II)-Sr(II) Cyclo-Tetraphosphates(V). *J. Therm. Anal. Calorim.* **2002**, *68*, 75.
(2) Trojan, M.; Šulcová, P. The Thermal Analysis of Binary Zn(II)-Sr(II) Cyclo-tetraphosphates. *J. Therm. Anal. Calorim.* **2000**, *60*, 215.
(3) Trojan, M.; Šulcová, P.; MoŠner, P. The synthesis of binary zinc(II)-nickel(II) cyclo-tetraphosphates as new special pigments. *Dyes Pigm.* **2000**, *44*, 161.
(4) Trojan, M.; Palme, J. New colour compounds binary cyclo-tetraphosphates $Mn_{2-x}Co_xP_4O_{12}$ and $Zn_{2-x}Co_xP_4O_{12}$. *Dyes Pigm.* **1993**, *22*, 173.
(5) Brandová, D.; Trojan, M.; Arnold, M.; Paulik, F. Thermal study of decomposition of $Cu_{1/2}Mg_{1/2}(H_2PO_4)_2$.0.5 $H_2O$. *J. Therm. Anal. Calorim.* **1990**, *36*, 677.
(6) Trojan, M.; Šulcová, P. Binary Cu(II)-Mn(II) cyclo-tetraphosphates. *Dyes Pigm.* **2000**, *47*, 291.
(7) Trojan, M.; Beneš, L. Binary cyclo-tetraphosphates $Mg_{2-x}Zn_xP_4O_{12}$and $Mg_{2-x}Ca_xP_4O_{12}$. *Mater. Res. Bull.* **2000**, *26*, 693.
(8) Trojan, M.; Brandová, D. A study of the thermal preparation of c-$Cd_{4/3}Ca_{2/3}P_4O_{12}$. *Thermochim. Acta* **1990**, *160*, 349.
(9) Gunsser, W.; Fruehauf, D.; Rohwer, K.; Zimmermann, A.; Wiedenmann, A. Synthesis and magnetic properties of transition metal cyclotetraphosphates $M_2P_4O_{12}$ (M = Mn, Co, Ni, Cu). *J. Solid State Chem.* **1989**, *82*, 43.
(10) Samuskevich, V. V.; Lukyanchenko, O. A.; Samuskevich, L. N. Disproportionation of $Zn(H_2PO_4)_2 \cdot 2H_2O$ Crystals (Topochemical Particularities. *Ind. Eng. Chem. Res.* **1997**, *36*, 4791.
(11) Boonchom, B.; Youngme, S.; Danvirutai, C. A rapid co-precipitation and non-isothermal decomposition kinetics of new binary $Mn_{0.5}Co_{0.5}(H_2PO_4)_2 \cdot 2H_2O$. *Solid State Sci.* **2008**, *10*, 129. and Reference therein.
(12) Boonchom, B.; Danvirutai, C. Rapid Coprecipitation and Non-Isothermal Decomposition Kinetics of New Binary $Mn_{0.5}Cu_{0.5}(H_2PO_4)_2 \cdot 1.5H_2O$. *Ind. Eng. Chem. Res.* **2008**, *47*, 2941.
(13) Brandová, D.; Trojan, M.; Paulik, F.; Paulik, J.; Arnold, M. Study of the thermal dehydration of $Mn_{1/2}Ca_{1/2}(H_2PO_4)_2.2H_2O$. *J. Therm. Anal. Calorim.* **1990**, *36*, 881.
(14) Trojan, M.; Brandová, D. Study of thermal dehydration of $Mn_{0.5}Mg_{0.5}(H_2PO_4)_2 \cdot 4H_2O$. *Thermochim. Acta* **1990**, *161*, 11.
(15) Trojan, M.; Palme, J.; Mazan, P. Binary cobalt(II)-copper(II) cyclo-tetraphosphates as new colour compounds. *Thermochim. Acta* **1990**, *224*, 177.
(16) Vlaev, L.; Nedelchev, N.; Gyurova, K.; Zagorcheva, M. A comparative study of non-isothermal kinetics of decomposition of calcium oxalate monohydrate. *J. Anal. Appl. Pyrolysis* **2008**, *81*, 253.
(17) Vlase, T.; Vlase, G.; Birta, N.; Doca, N. Comparative results of kinetic data obtained with different methods for complex decomposition steps. *J. Therm. Anal. Calorim.* **2007**, *88*, 631.
(18) Vlase, G.; Vlase, T.; Tudose, R.; Costişor, O.; Doca, N. Kinetic of decomposition of some complexes under non-isothermal conditions. *J. Therm. Anal. Calorim.* **2007**, *88*, 637.
(19) Vlaev, L. T.; Georgieva, V. G.; Genieva, S. D. Products and kinetics of non-isothermal decomposition of vanadium(IV) oxide compounds. *J. Therm. Anal. Calorim.* **2007**, *88*, 805.
(20) Vlaev, L. T.; Georgieva, V. G.; Gospodinov, G. G. Kinetics of isothermal decomposition of $ZnSeO_3$ and $CdSeO_3$. *J. Therm. Anal. Calorim.* **2005**, *79*, 163.
(21) Vlaev, L. T.; Tavlieva, M. P. Structural and thermal studies on the solid products in the system $MnSeO_3$-$SeO_2$-$H_2O$. *J. Therm. Anal. Calorim.* **2007**, *90*, 385.
(22) Chunxiu, G.; Yufang, S.; Donghua, C. Comparative method to evaluate reliable kinetic triplets of thermal decomposition reactions. *J. Therm. Anal. Calorim.* **2004**, *76*, 203.
(23) Boonchom, B.; Youngme, S.; Srithanratana, T.; Danvirutai, C. Synthesis of $AlPO_4$ and kinetics of thermal decomposition of $AlPO_4 \cdot H_2O$-H4 precursor. *J. Therm. Anal. Calorim.* **2008**, *91*, 551.
(24) Boonchom, B.; Danvirutai, C. Synthesis of $MnNiP_2O_7$ and Nonisothermal Decomposition Kinetics of a New Binary $Mn_{0.5}Ni_{0.5}HPO_4 \cdot H_2O$ Precursor Obtained from a Rapid Coprecipitation at Ambient Temperature. *Ind. Eng. Chem. Res.* **2008**, *46*, 9071.
(25) Boonchom, B.; Maensiri, S.; Youngme, S.; Danvirutai, C. A simple synthesis and room temperature magnetic properties of new binary $Mn_{0.5}Fe_{0.5}(H_2PO_4)_2 \cdot xH_2O$ obtained from a rapid co-precipitation at ambient temperature. *Solid State Sci.* **2009**, *11*, 485.
(26) Koleva, V.; Mehandjiev, D./initials>. Characterization of $M(H_2PO_4)_2 \cdot 2H_2O$ (M = Mn, Co, Ni) and their in situ thermal decomposition by magnetic measurements. *Mater. Res. Bull.* **2006**, *41*, 469.
(27) Koleva, V. Effenberger, H. Crystal chemistry of $M[PO_2(OH)_2]_2 \cdot 2H_2O$ compounds (M = Mg, Mn, Fe, Co, Ni, Zn, Cd): Structural investigation of the Ni, Zn and Cd salts. *J. Solid State Chem.* **2007**, *180*, 966, and references therein.
(28) Ramakrishnan, V.; Aruldhas, G.; Bigotto, A. Vibrational spectra of Cu(II) and Co(II) tetrametaphosphates. *Infrared Phys.* **1985**, *25*, 665.
(29) Halawy, S. A.; Fouad, N. E.; Mohamed, M. A.; Zaki, M. I. Kinetic and Thermodynamic Parameters of the Decomposition of Chromium Chromate in Different Gas Atmospheres. *J. Therm. Anal. Calorim.* **2005**, *82*, 671.
(30) Abu-Eittah, R. H.; ZaKi, N. G.; Mohamed, M. M. A.; Kamel, L. T. Kinetics and thermodynamic parameters of the thermal decomposition of bis(imipraminium)tetrachlorocuprate, bis(imipraminium)tetrachloromercurate and imipraminium reineckate. *J. Anal. Appl. Pyrolysis* **2006**, *77*, 1.
(31) Ma, H. X.; Song, J. R.; Zhao, F. Q.; Hu, R. Z.; Xiao, H. M. Nonisothermal Decomposition Kinetics and Computational studies on the Properties of 2,4,6,8-Tetranitro-2,4,6,8-tetraazabicyclo[3,3,1]onan-3,7-dione (TNPDU). *J. Phys. Chem. A* **2007**, *111*, 8642.
(32) Head, C.; Smith, A. C. K. *Applied Physical Chemistry*; McMilan Press: London, 1982; p 473.
(33) Šesták, J. J. *Thermodynamical properties of solids*; Academia: Prague, 1984.
(34) Young, D. *Decomposition of solids*; Pergamon Press: Oxford, 1966.
(35) Turmanova, S.Ch.; Genieva, S. D.; Dimitrova, A. S.; Vlaev, L. T. Non-isothermal degradation kinetics of filled with rise husk ash polypropene composites. *Express Polym. Lett.* **2008**, *2*, 133.
(36) Coats, W.; Redfern, J. P. Kinetic Parameters from Thermogravimetric Data. *Nature (London)* **1964**, *201*, 68.
(37) Madhysudanan, P. M.; Krisnan, K.; Ninan, K. N. New equations for kinetic analysis of non-isothermal reactions. *Thermochim. Acta* **1993**, *221*, 13.
(38) Tang, W.; Liu, Y.; Zang, H.; Wang, C. New approximate formula for Arrhenius temperature integral. *Thermochim. Acta* **2003**, *408*, 39.
(39) Boonchom, B. Kinetics and Thermodynamic Properties of the Thermal Decomposition of Manganese Dihydrogenphosphate Dihydrate. *J. Chem. Eng. Data* **2008**, *53*, 1533.
(40) Cordes, H. M. Preexponential factors for solid-state thermal decomposition. *J. Phys. Chem.* **1968**, *72*, 2185.
(41) Criado, J. M.; Pérez-Maqueda, L. A.; Sánchez-Jiménez, P. E. Dependence of the preexponential factor on temperature. *J. Therm. Anal. Calorim.* **2005**, *82*, 671.

Received for review March 28, 2009. Accepted September 3, 2009. This work is financially supported by the Thailand Research Fund (TRF) and the Commission on Higher Education (CHE): Research Grant for New Scholar and King Mongkut's Institute of Technology Ladkrabang Research (KMITL Research), Ministry of Education, Thailand.

JE900310M